Supplementary Information

Centrosymmetric RbSnF$_2$NO$_3$ vs. Noncentrosymmetric Rb$_2$SbF$_3$(NO$_3$)$_2$

Lei Wang, [†] Hongmei Wang, [†] Die Zhang, [†] Daojiang Gao, [†] Jian Bi, [†] Ling Huang, *[†] and Guohong Zou*[‡]

[†] College of Chemistry and Materials Science, Sichuan Normal University, Chengdu, 610068, P. R. China.

[‡] College of Chemistry, Sichuan University, Chengdu, 610064, P. R. China.

E-mail: huangl026@sina.com; zough@scu.edu.cn

Table of contents

Section S1. Materials and Methods

Instruments The diffraction data acquisition of compounds $RbSnF_2NO_3$ and $Rb_2SbF_3(NO_3)_2$ were implemented by graphite-monochromated Mo Kα radiation (λ=0.71073 Å) integrating with the SAINT program on a Bruker D8 Venture detector at a temperature of 150(2) K. SHELX-2014 program was applied to establish the crystal structures by direct method, and structures were further refined on F^2 through the full-matrix least-squares method. [1] The program PLATON was used to examine possible additional symmetry and no higher symmetry could be found. [2] One possession disorder oxygen atom exits in $Rb_2SbF_3(NO_3)_2$, which is common for the single crystals. The crystallographic parameters as well as refinement information for two title compounds were given in table 1. The other structural data including the atomic coordinates, the selected bond distances (Å) and angles (deg.) were given in Tables S1-S4.The powder X-ray diffraction patterns to confirm the purity of $Rb_2SbF_3(NO_3)_2$ and $RbSnF_2NO_3$ powder samples were acquired on an automated Smart lab diffractometer equipped with Cu-Kα radiation (λ=1.540598 Å). The measuring parameters are set as: angular ranging from 5° to 70° (2θ) with a fixed counting time of 0.2 s and a step size of 0.08° at room temperature. The IR transmission of title compounds were carried out at room temperature in the 400-4000 cm^{-1} wavenumber range on a Vertex 70 Fourier transform infrared (FT-IR) spectrometer. KBr was used as background and the powdery specimens were equally mixed with dehydrated KBr and ground into fine powder with a mass proportion of 1:100, and then prepared samples were put into transparent slices for the measurements. The thermal behaviors of the ground polycrystalline samples were conducted with a NETZSCH SET-449C instrument. Approximate 14-17 mg of crystal powders were enclosed into Al_2O_3 crucibles and heated in a temperature range of 30-800 ℃with the heating rate of 10 ℃/min under a constant flow of nitrogen gas. A UV-2600, Shimadzu spectrophotometer equipped with an integrating sphere at 185-800 nm was used to test optical diffuse-reflectance spectra, which can determine the cut-off edge of the title compounds. The reflectance spectra were carried out at ambient temperature using dried $BaSO_4$ plate as a 100% reference comparison standard. The reflection spectra were converted into absorption spectra through the Kubelka-Munk function a/S $= (1-R)^2/2R$, in this equation, a is the absorption coefficient, S stands for the scattering coefficient that is essentially wavelength-independent when the particle size is larger than 5 μm, and R is the

reflectance. The powder SHG effects of the compound $Rb_2SbF_3(NO_3)_2$ were performed by employing the method of Kurtz-Perry under a 1064 nm laser, which were radiated by a Q-switched Nd:YAG laser at ambient temperature. [3] Since the powder SHG effect is definitely related to particle size, the samples of $Rb_2SbF_3(NO_3)_2$ and a reference of KH_2PO_4 (KDP) were ground, then sieved into the following six discrete particle size ranges: 25-45, 45-58, 58-75, 75-106, 106-150, 150-212 μm, which were loaded between glass slides and then pressed into respective sample rubber rings. $Rb_2SbF_3(NO_3)_2$ and KDP powders were sieved into the same particle size to assume the SHG effect. A photomultiplier tube was used to collect the signal of the frequency-doubled output emitted from the microcrystalline samples. The first-principles calculations for $Rb_2SbF_3(NO_3)_2$ and $RbSnF_2NO_3$ crystals were based on their single crystal structure data. The electronic structures, optical properties and density of states (DOS) were obtained by the plane-wave pseudopotential method implemented in the CASTEP package on the basis of the density functional theory (DFT).[4] Meanwhile the Perdew-Burke-Brnzerhof (PBE) functional was chosen to treat the exchange-correlation potential within the generalized gradient approximation (GGA).[5] The cutoff energy for plane wave functions were set as 850 eV for both compounds and the numerical integration of the Brillouin zones were performed using 3×5×3 and 1×3×3 Monkhorst-Pack k-point for $Rb_2SbF_3(NO_3)_2$ and $RbSnF_2NO_3$, respectively. The employed convergence benchmark was $1.0×10^{-6}$ eV/atom. The connections between the valence electrons and the ionic cores were demonstrated using optimized norm-conserving pseudopotentials in Kleinman–Bylander form.[6]

Table S1. Fractional atomic coordinates and isotropic or equivalent isotropic displacement parameters ($Å^2$) for $RbSnF_2NO_3$.

atom	x	y	z	Ueq ($Å^2$)	BVS
Sn1	0.535133 (19)	0.5	0.28349 (4)	0.02474 (11)	1.9907
Rb1	0.81330 (3)	0.5	0.31182 (6)	0.02688 (13)	1.2153
F1	0.66970 (16)	0.5	0.4958 (4)	0.0284 (5)	1.1036
F2	0.5	0.7344 (4)	0.5	0.0279 (5)	1.1645
O1	0.64698 (15)	−0.2007 (4)	0.0576 (3)	0.0326 (5)	1.9762
O2	0.5839 (2)	0.0	0.2427 (5)	0.0321 (7)	1.9151
N1	0.6261 (2)	0.0	0.1176 (5)	0.0244 (7)	4.8768

Table S2. Fractional atomic coordinates and isotropic or equivalent isotropic displacement parameters (Å^2) for Rb$_2$SbF$_3$(NO$_3$)$_2$.

atom	x	y	z	Ueq (Å^2)	BVS
Sb1	0.6116 (4)	0.7624 (4)	0.2975 (3)	0.0290 (9)	3.023
Sb2	0.7810 (3)	0.4707 (4)	0.8247 (3)	0.0264 (8)	2.911
Rb1	0.3555 (6)	0.7084 (6)	0.5102 (4)	0.0323 (12)	1.298
Rb2	0.6303 (6)	1.1788 (7)	0.0681 (4)	0.0347 (13)	1.185
Rb3	1.0507 (5)	0.4555 (7)	0.6505 (4)	0.0302 (11)	1.220
Rb4	1.0574 (5)	0.4659 (7)	1.1318 (4)	0.0313 (11)	1.171
F1	0.825 (3)	0.291 (4)	0.717 (2)	0.036 (7)	1.096
F2	0.818 (3)	0.281 (4)	0.944 (3)	0.035 (7)	1.149
F3	0.957 (3)	0.522 (4)	0.870 (3)	0.035 (7)	1.140
F4	0.478 (4)	0.824 (5)	0.158 (3)	0.046 (9)	1.068
F5	0.510 (3)	0.875 (4)	0.388 (3)	0.040 (8)	1.218
F6	0.674 (3)	1.007 (4)	0.292 (2)	0.033 (7)	1.283
N1	1.117 (6)	−0.087 (7)	0.659 (5)	0.045 (11)	4.931
N2	0.742 (5)	0.683 (6)	1.055 (4)	0.034 (9)	5.162
N3	0.766 (5)	0.713 (6)	0.573 (4)	0.034 (9)	5.059
N4	0.417 (6)	0.434 (8)	0.233 (5)	0.049 (12)	5.727
O1	1.126 (5)	−0.174 (6)	0.571 (4)	0.045 (11)	2.151
O2	1.142 (5)	−0.164 (6)	0.762 (4)	0.046 (10)	1.859
O3	1.078 (5)	0.069 (6)	0.648 (5)	0.064 (14)	1.986
O4	0.832 (4)	0.664 (5)	1.008 (3)	0.034 (9)	2.079
O5	0.654 (4)	0.580 (5)	1.030 (4)	0.040 (9)	2.011
O6	0.746 (4)	0.814 (5)	1.120 (4)	0.041 (10)	2.080
O7	0.676 (4)	0.610 (5)	0.544 (4)	0.041 (10)	1.833
O8	0.776 (4)	0.841 (5)	0.503 (3)	0.038 (10)	1.943
O9	0.846 (4)	0.697 (5)	0.666 (3)	0.034 (8)	2.226
O10	0.439 (6)	0.530 (8)	0.317 (5)	0.079 (14)	2.341
O11	0.320 (7)	0.388 (9)	0.175 (7)	0.096 (18)	2.255
O12	0.520 (12)	0.362 (14)	0.239 (10)	0.071 (19)	1.968

Table S3. Selected Bond lengths (Å) and angles (deg) for RbSnF$_2$NO$_3$.

Sn1—F1	2.027 (2)	Rb1—O2^{ii}	2.967 (3)
Sn1—F2	2.2001 (14)	Rb1—O1^{vi}	3.092 (2)
Sn1—F2^{i}	2.2001 (14)	Rb1—O1^{vii}	2.964 (2)
Sn1—O2	2.8416 (1)	Rb1—O1^{viii}	3.092 (2)
Rb1—F1^{iii}	2.9960 (11)	Rb1—O1^{ix}	2.964 (2)
Rb1—F2^{iv}	2.9883 (12)	O2—N1	1.266 (5)
O1—N1^{vii}	1.246 (3)	F2—Sn1—F1	84.74 (6)
F2^{i}—Sn1—F1	84.74 (6)	O1^{viii}—Rb1—F2^{iv}	76.73 (4)
F2^{i}—Sn1—F2	70.32 (10)	O1^{vii}—Rb1—F2^{v}	116.77 (6)
F1^{ii}—Rb1—F1	75.37 (5)	O1^{vi}—Rb1—F2^{iv}	96.17 (4)
F1^{ii}—Rb1—F1^{iii}	128.81 (8)	O1^{vi}—Rb1—F2^{v}	76.73 (4)
F2^{iv}—Rb1—F1^{iii}	108.68 (6)	O1^{viii}—Rb1—O2^{ii}	135.91 (7)
F2^{v}—Rb1—F1^{iii}	56.91 (6)	O1^{vii}—Rb1—O2^{ii}	129.85 (6)
F2^{iv}—Rb1—F2^{v}	57.40 (8)	O1^{vii}—Rb1—O1^{ix}	66.15 (9)
O2^{ii}—Rb1—F1^{ii}	65.79 (4)	O1^{vii}—Rb1—O1^{vi}	70.90 (6)
O2^{ii}—Rb1—F1^{iii}	65.79 (4)	O1^{viii}—Rb1—O1^{ix}	70.90 (6)
O2^{ii}—Rb1—F1	72.57 (7)	Rb1—F1—Sn1	111.44 (10)
O2^{ii}—Rb1—F2^{iv}	59.25 (5)	Rb1^{iii}—F1—Sn1	103.53 (5)
O1^{ix}—Rb1—F1^{ii}	72.37 (6)	Rb1^{ii}—F1—Rb1	104.63 (5)
O1^{vii}—Rb1—F1^{iii}	72.37 (6)	Sn1^{x}—F2—Sn1	109.68 (10)
O1^{vi}—Rb1—F1^{iii}	93.43 (6)	Rb1^{xi}—F2—Sn1^{x}	99.432 (9)
O1^{vii}—Rb1—F1^{ii}	132.97 (6)	Rb1^{ii}—F2—Sn1	99.432 (9)
O1^{vi}—Rb1—F1^{ii}	133.83 (6)	Rb1^{xi}—F2—Sn1	112.905 (9)
O1^{viii}—Rb1—F1^{ii}	93.43 (6)	Rb1^{ii}—F2—Rb1^{xi}	122.60 (8)
O1^{ix}—Rb1—F1^{iii}	132.97 (6)	N1—O2—Rb1^{iii}	123.4 (2)
O1^{vi}—Rb1—F1	142.04 (6)	N1^{vii}—O1—Rb1^{viii}	97.79 (18)
O1^{vii}—Rb1—F1	71.15 (6)	O1^{vii}—N1—O2	119.53 (16)
O1^{ix}—Rb1—F2^{v}	167.04 (5)	O1—N1—O2	119.53 (16)
O1^{ix}—Rb1—F2^{iv}	116.77 (6)	O1—N1—O1^{vii}	120.9 (3)

Symmetry codes: (i) −x+1, −y+1, −z+1; (ii) −x+3/2, y+1/2, −z+1; (iii) −x+3/2, y−1/2, −z+1; (iv) −x+3/2, −y+3/2, −z+1; (v) x+1/2, y−1/2, z; (vi) x, y+1, z; (vii) −x+3/2, −y+1/2, −z; (viii) x, −y, z; (ix) −x+3/2, y+1/2, −z; (x) −x+1, y, −z+1; (xi) x−1/2, y+1/2, z.

Table S4. Selected Bond lengths (Å) and angles (deg) for $Rb_2SbF_3(NO_3)_2$.

Sb2—F3	1.93 (3)	Rb2—F2^{xii}	2.92 (3)
Sb2—F2	1.94 (3)	Rb2—O12^{viii}	2.92 (11)
Sb2—F1	1.97 (3)	Rb2—O6^{xiii}	2.99 (4)
Sb2—O4	2.50 (4)	Rb2—O2^{xiv}	3.01 (5)
Sb1—F5	1.92 (3)	F2—Rb2^{iii}	2.92 (3)
Sb1—F4	1.94 (3)	F2—Rb4^{ii}	2.96 (3)
Sb1—F6	1.95 (3)	F3—Rb4^{i}	3.30 (3)
Rb3—O3	2.88 (4)	O9—Rb4^{i}	3.05 (4)
Rb3—O9	2.94 (4)	O4—N2	1.26 (6)
Rb3—O1^{v}	2.95 (4)	O4—Rb4^{i}	3.19 (4)
Rb3—O2^{viii}	3.16 (5)	O1—N1	1.23 (7)
Rb3—N1^{viii}	3.47 (5)	O1—Rb3^{vii}	2.95 (4)
Rb4—O11^{ix}	2.89 (7)	O8—N3	1.27 (5)
Rb4—F2^{i}	2.96 (3)	O8—Rb1^{vi}	3.07 (4)
Rb4—O2^{i}	2.96 (5)	O2—N1	1.29 (7)
Rb4—F3^{ii}	3.30 (3)	N4—O11	1.17 (8)
Rb4—O3^{i}	3.36 (6)	N4—O10	1.18 (7)
Rb4—N1^{i}	3.49 (6)	N4—O12	1.24 (12)
Rb1—F5	2.78 (3)	N1—O3	1.23 (7)
Rb1—F6^{iv}	2.82 (3)	O3—Rb4^{ii}	3.36 (6)
Rb1—F1^{vi}	2.93 (3)	O3—Rb3^{vii}	3.48 (6)
Rb1—Sb1^{iv}	3.952 (6)	F1^{vi}—Rb1—Sb1^{iv}	128.5 (6)
F3—Sb2—F2	86.2 (13)	F5^{iv}—Rb1—Sb1^{iv}	27.8 (7)
F3—Sb2—F1	84.8 (14)	O7—Rb1—Sb1^{iv}	79.7 (6)
F2—Sb2—F1	84.9 (13)	F4^{xi}—Rb2—F6	164.8 (11)
F2—Sb2—Rb3	106.5 (10)	F4^{xi}—Rb2—F2^{xii}	68.5 (10)
Rb2^{iii}—Sb2—Rb1^{iv}	105.17 (13)	O9—N3—O8	119 (5)
F5—Sb1—F4	85.6 (15)	O7—N3—O8	119 (4)
F5—Sb1—F6	82.8 (14)	F4—Sb1—Rb3^{v}	122.4 (12)
F4—Sb1—F6	87.4 (14)	O3—Rb3—O2^{viii}	150.3 (14)

Symmetry codes: (i) −x+2, y+1/2, −z+2; (ii) −x+2, y−1/2, −z+2; (iii) x, y−1, z+1; (iv) −x+1, y−1/2, −z+1; (v) −x+2, y+1/2, −z+1; (vi) −x+1, y+1/2, −z+1; (vii) −x+2, y−1/2, −z+1; (viii) x, y+1, z; (ix) x+1, y, z+1; (x) x−1, y+1, z; (xi) −x+1, y+1/2, −z; (xii) x, y+1, z−1; (xiii) x, y, z−1; (xiv) −x+2, y+3/2, −z+1; (xv) x+1, y−1, z; (xvi) x, y−1, z; (xvii) −x+2, y−3/2, −z+1; (xviii) −x+1, y−1/2, −z; (xix) x−1, y, z−1; (xx) x, y, z+1.

Table S5. Calculation of dipole moment for NO_3, SbO_2F_3, SbO_3F_3, RbO_5F_3, RbO_5F_4, RbO_7F_3 and RbO_6F_3 polyhedra and net dipole moment for a unit cell in $Rb_2SbF_3(NO_3)_2$. (D = Debyes).

Rb₂SbF₃(NO₃)₂				
Polar unit (a unit cell)	Dipole moment (D)			
	x-component	y-component	z-component	total magnitude
NO_3	0.513648436	0.234558814	0.191112285	0.596134598
	0.108485631	-0.157171827	0.081992262	0.207833699
	-0.108485631	-0.157171827	-0.081992262	0.207833699
	0.227026782	-0.619199226	-0.5539297	0.861270546
	-0.504323787	0.234173996	-0.191065945	0.587950795
	0.862960812	0.978223436	2.826191867	3.112713113
	-0.153060783	-0.557626404	0.479223504	0.751019291
	-0.937774147	1.031641798	-2.95170051	3.264389844
total	0.008477313	0.98742876	-0.118176237	0.994511
SbO_2F_3	-18.00575606	4.576773595	-5.524643663	19.38235784
	18.02497973	4.57187686	5.528761606	19.40023601
total	0.01922367	9.148650455	0.004117943	9.148671579
SbO_3F_3	7.671279642	-15.50425804	1.25043272	17.3434175
	-7.673115176	-15.50350597	-1.248829415	17.34344166
total	-0.001835534	-31.00776401	0.001603305	31.00776411
RbO_5F_3	-2.969476493	-1.516763083	1.490241888	3.652284461
	2.969696696	-1.516572524	-1.490397569	3.652447891
total	0.000220203	-3.033335607	-0.000155681	3.033335619
RbO_5F_4	-1.532447842	1.921428942	-0.455412973	2.499537266
	1.532030836	1.920925535	0.455560068	2.498921441
total	-0.000417006	3.842354477	0.000147095	3.842354502
RbO_7F_3	0.677633926	-1.091620233	3.280630448	3.523259657
	-0.67702583	-1.089989837	-3.279237974	3.521341152
total	0.000608096	-2.18161007	0.001392474	2.181610599
RbO_6F_3	2.863556564	-1.362563963	-0.80970568	3.272943635
	-2.60569618	-1.851204741	0.402707331	3.221612139
total	0.257860384	-3.213768704	-0.406998349	3.249684433
Net dipole moment	0.284137	-25.458	-0.51807	25.4649
Cell Volume	919.7 Å³			
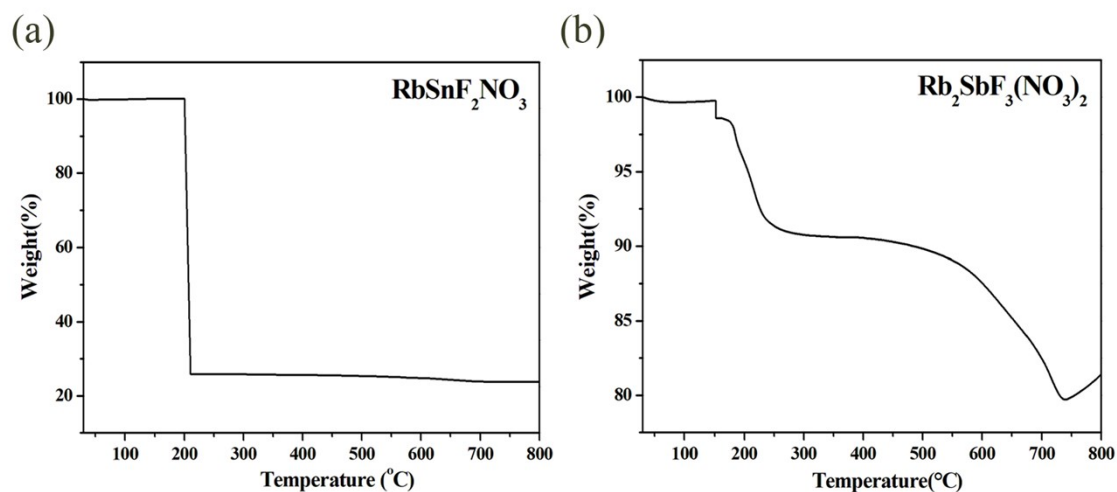
Fig. S1 TGA curves of (a) $RbSnF_2NO_3$ and (b) $Rb_2SbF_3(NO_3)_2$ under N_2 atmosphere.
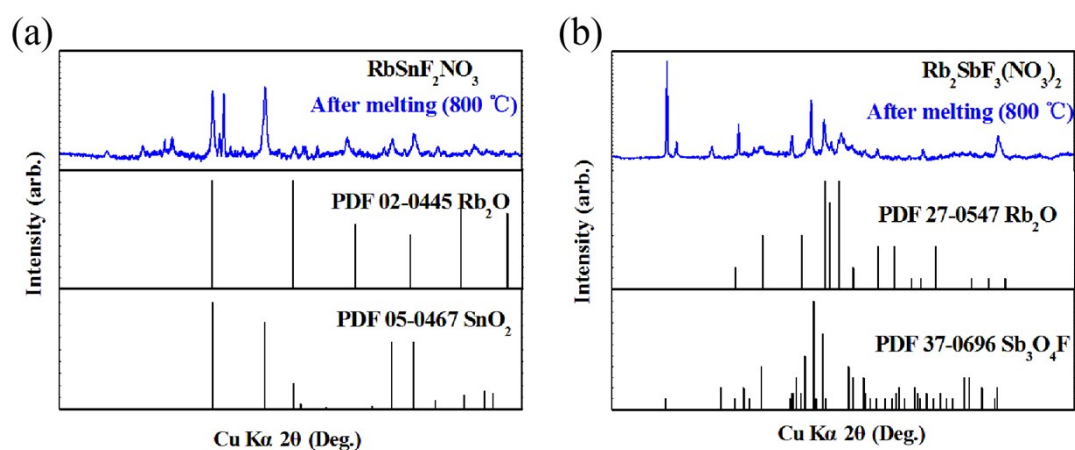
Fig. S2 XRD patterns of the residues of TGA for (a) $RbSnF_2NO_3$ and (b) $Rb_2SbF_3(NO_3)_2$.
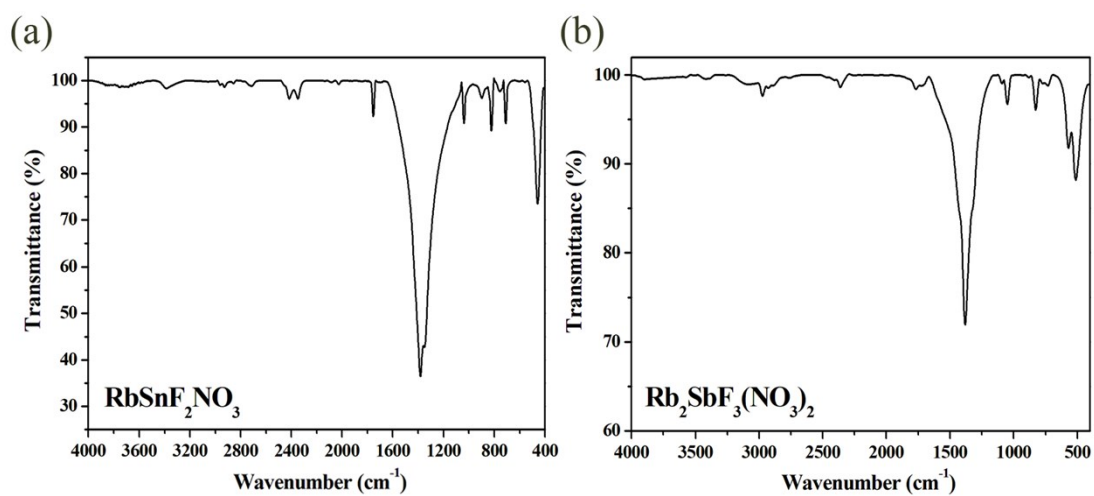
Fig. S3 The IR spectra of (a) $RbSnF_2NO_3$ and (b) $Rb_2SbF_3(NO_3)_2$.
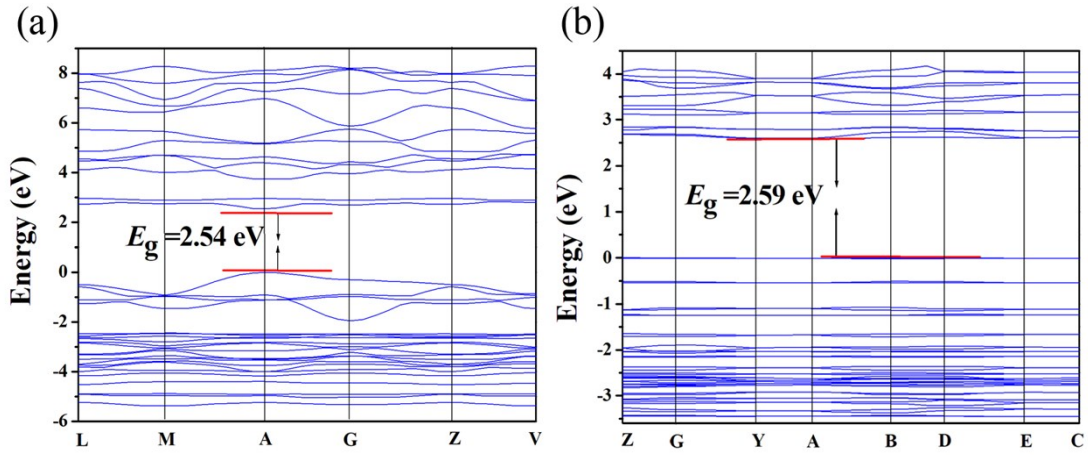
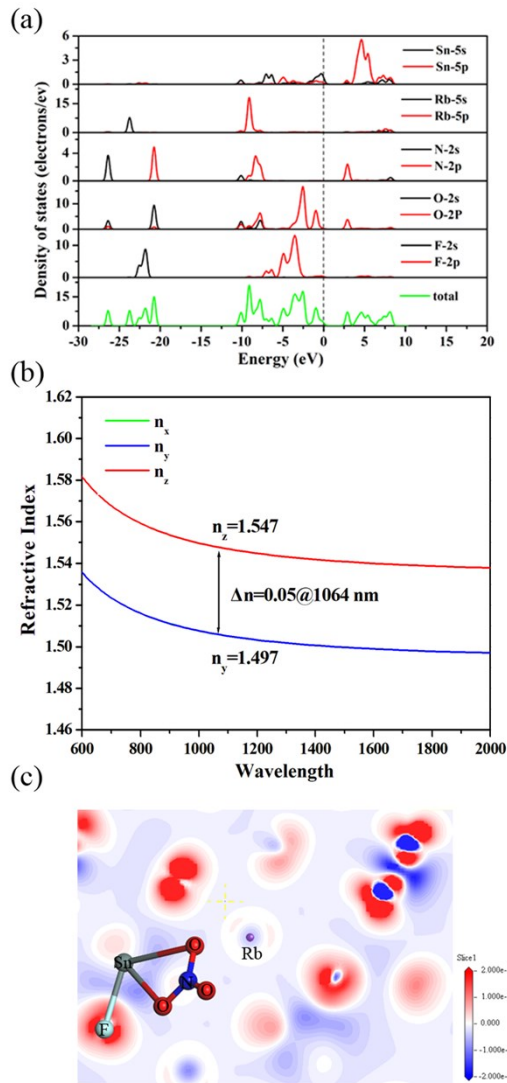**Fig. S4** Calculated band structures of (a) $RbSnF_2NO_3$ and (b) $Rb_2SbF_3(NO_3)_2$.

Fig. S5 The theoretical calculations of $RbSnF_2NO_3$. (a) Total and partial DOS of states for $RbSnF_2NO_3$, the Fermi level is normalized to 0 eV; (b) the calculated birefringence curves for $RbSnF_2NO_3$; (c) the electron-density difference map for $RbSnF_2NO_3$.

References

(1) Sheldrick, G.M. A short history of SHELX-2014, *Acta Crystallogr.* 2008, 64, 112-122.

(2) Spek, A. L. Single-crystal structure validation with the program PLATON. *J. Appl. Crystallogr.* **2003**, *36*, 7-13.

(3) Kurtz, S. K.; Perry, T. T. A powder technique for the evaluation of nonlinear optical materials. *J. Appl. Phys.* **1968**, *39*, 3798-3813.

(4) Segall, M. D.; Lindan, P. J. D.; Probert, M. J. First-principles simulation: ideas, illustrations and the CASTEP code. *J. Phys. Condens. Matter.* **2002**, *14*, 2717.

(5) Perdew, J. P.; Burke, K.; Ernzerhof, M. Generalized gradient approximation made simple, *Phys. Rev. Lett.* **1996**, *77*, 3865-3868.

(6) Vanderbilt, D. Soft self-consistent pseudopotentials in a generalized eigenvalue formalism, *Phys. Rev. B.* **1990**, *41*, 7892.